ELSEVIER

Carbohydrate Research 337 (2002) 1745–1756

CARBOHYDRATE RESEARCH

www.elsevier.com/locate/carres

NMR studies of molybdate complexes of D-*erythro*-L-*manno*-octose and D-*erythro*-L-*gluco*-octose and their alditols

Mária Matulová,* Zuzana Hricovíniová

Institute of Chemistry, Slovak Academy of Sciences, SK-842 38 Bratislava, Slovakia

Received 25 April 2002; accepted 26 June 2002

Abstract

Different amounts and various types of bis-dinuclear tetradentate molybdate complexes of D-*erythro*-L-*manno*-octose, D-*erythro*-L-*gluco*-octose, D-*erythro*-L-*manno*-octitol and D-*erythro*-L-*gluco*-octitol were characterized by ^{1}H and ^{13}C NMR spectroscopy in aqueous solutions. Detailed analysis of $^{1}H-^{1}H$ coupling constants and NOEs, together with chemical shifts, allowed characterization of the different isomers of these complexes. © 2002 Elsevier Science Ltd. All rights reserved.

Keywords: D-*erythro*-L-*manno*-Octose; D-*erythro*-L-*gluco*-Octose; D-*erythro*-L-*manno*-Octitol; D-*erythro*-L-*gluco*-Octitol; Mo^{VI} complexes; NMR spectroscopy

1. Introduction

The interaction of metal ions with carbohydrates has been a topic of interest for a number of years. One of the major achievements in this field is the discovery of the isomerization of the carbohydrate carbon skeleton upon formation of molybdate complexes of aldoses.[1] The selective Bílik's C-2 epimerization reaction, during which C-1/C-2 transposition occurs, is preceded by the formation of active dinuclear tetradentate molybdate complexes between aldoses and molybdate.[1–4] Systematic studies of these complexes in aqueous solutions include a variety of monosaccharides, their derivatives as well as alditols.[4–11] It was assumed that the aldose adopts the acyclic aldehyde form in the molybdate complex. In this transition state, the linkage between C-2 and C-3 splits while a new one is simultaneously formed between C-3 and C-1.[2] Complexes with the cyclic form of aldose are not active in the epimerization reaction as these complexes fix Mo^{VI} ions which results in a decrease in the reaction rate.[3] According to this observation, it was found that the OH-2,3 configuration of the cyclic form of higher aldoses (C-5–C-7) is a key parameter determining the prevalence of Mo^{VI} complexes with the cyclic or acyclic form of aldoses in individual homomorphous series. Thus, aldoses with the *erythro* arrangement of OH-2,3 (cis orientation) afford molybdate complexes predominantly in the cyclic form. The aldoses of the *lyxo* homomorphous series form complexes mainly with furanose structures[11] and those of *ribo* homomorphous series with pyranose structures.[6] Only a small amount of complexes with the acyclic form of the aldose were detected in both series.[4,6] Aldoses with the *threo* arrangement at OH-2,3 (trans orientation, arabinose and xylose homomorphous series) form complexes exclusively in their acyclic forms.[4,6] Aldotetroses and 5-deoxy-aldopentoses afford Mo^{VI} complexes exclusively in their acyclic forms.[7] In all cases, the $[Mo_2O_7]^{2-}$ dinuclear molybdate core is formed by two octahedra sharing a face. Previous data also indicated that some dinuclear tetradentate molybdate complexes of both alditols and acyclic forms of aldoses form pairs of isomers.[6,7,10,12]

Early studies of molybdate complexes of D-*erythro*-L-*manno*-octose (**1**) and D-*erythro*-L-*gluco*-octose (**2**) showed the presence of signals originating from both pyranose and furanose free forms in their NMR spec-

* Corresponding author
E-mail address: matulova@chisg1.univ-bpclermont.fr (M. Matulová).

PII: S0008-6215(02)00177-5

tra. In addition, resonances from aldooctoses chelated in various types of molybdate complexes were observed as well.[13] However, structures of these complexes were not fully characterized. In the present report, structures of various types of Mo^{VI} complexes of both octoses **1** and **2** are characterized and compared with complexes of the corresponding alditols.

2. Experimental

Deuterium oxide solutions of saccharide and ammonium molybdate $(NH_4)_6MoO_7O_{24}{\cdot}4\ H_2O$ in a 1:4 mol ratio, respectively, were measured on Bruker Avance DPX 300 MHz spectrometer at 310 K. Measurements were performed in a 5 mm multinuclear inverse probe with z-gradients and in 5 mm QNP probe. Sodium 3-(trimethylsilyl) propionate (TSP) (δ 0.0) was used as an internal standard in ^1H NMR spectra and acetone (δ 31.07) in ^{13}C NMR spectra. The following techniques were used for the assignment of NMR signals: DEPT, two-dimensional COSY,[14] one-dimensional transient NOESY,[15] HSQC,[16] and HMBC.[17] One-bond proton–carbon coupling constants ($^1J_{C-H}$) were measured by one-dimensional methods.[18] Solid state ^{13}C CP MAS spectra were measured at ambient temperature on Bruker Advance DSX 300 MHz spectrometer. Samples were spun in 4 mm ZrO_2 rotor at a rate of 4 kHz in a double air-bearing probe. Standard pulse sequence[19] was used with 4 μs proton 90° pulse, 1 ms contact time and 5 s repetition time and spectra were referenced to glycine carbonyl signal at δ 176.03.

D-*erythro*-L-*manno*-Octose (**1**) and D-*erythro*-L-*gluco*-octose (**2**), D-*erythro*-L-*manno*-octitol (**3**), D-*erythro*-L-*gluco*-octitol (**4**) were prepared as previously described.[13] Aqueous solutions of compounds **1**–**4** showed pH values 5.1–5.4 and these were slightly increased to 5.6–5.8 upon complexation with molybdate ions.

In the present work, we adopted the denomination of the complex types as follows:[12] Isomers $\mathbf{A_1}$, $\mathbf{A_2}$ include terminal primary CH_2OH group and its three vicinal OH groups with central *erythro* diol configuration in the sickle arrangement (characteristic for *arabino* arrangement). Isomers $\mathbf{E_1}$, $\mathbf{E_2}$ include the hydrated aldehyde group and its three vicinal OH groups with central *erythro* configuration in the sickle arrangement. Isomers $\mathbf{T_1}$, $\mathbf{T_2}$ hydrated aldehyde group and its three vicinal OH groups with central *threo* configuration in the zig-zag arrangement. Isomers $\mathbf{G_1}$, $\mathbf{G_2}$ include four internal vicinal OH groups of the *galacto* arrangement. The **Q**-type complex includes terminal primary CH_2OH and its three vicinal OH groups with central *threo* diol configuration in zig-zag arrangement.

3. Results and discussion

Aldotetroses up to aldoheptoses form various types of Mo^{VI} complexes and their structures depend upon the configuration of hydroxy groups in the molecule. Since four OH groups participate on complex formation, they can form only one binuclear tetradentate complex. However, aldooctoses have eight OH groups appropriate for the chelation and thus bis-dinuclear molybdate complexes might be formed with these monosaccharides. Signals due to various complex types of aldooctoses **1** and **2** with Mo^{VI}, as well as uncomplexed forms, were observed in high-resolution NMR spectra. The resonances in **1** and **2**, as well as in aldooctitols **3** and **4** (Table 1) were assigned by 2D HSQC and HMBC NMR techniques.

The D-*erythro*-L-*manno*-octitol symmetric molecule **3** offered two *arabino*-type sites suitable for formation of the sickle–sickle arrangements (two **A** types tetradentate dinuclear complexes) of the carbon chain. In the case of lower alditols (C-5–C-7), the **A** type complex at the *arabino* site was observed in the form of $\mathbf{A_1}$ and $\mathbf{A_2}$ isomers.[20] Each isomer showed characteristic chemical shifts and coupling constants (Table 1). Both proton and carbon signals originating from the CH_2OH group, involved in the complex, were found particularly characteristic. For example, H-5′ in the isomer $\mathbf{A_1}$ of arabinitol (δ 4.07) showed a characteristic splitting due to the coupling constants $^3J_{4,5'}$ 2.6 Hz, $^4J_{3,5'}$ 2.0 Hz and $^2J_{5,5'}$ 10.3 Hz in the ^1H NMR spectrum. At the same time, the signal for H-5 (δ 4.35) was in the form of a doublet ($^2J_{5,5'}$ 10.3 Hz). On the other hand, the complex multiplet at $\delta \approx 4.50$ due to H-5 and H-5′ signals was characteristic for the isomer $\mathbf{A_2}$. In addition, the ^{13}C chemical shift of the CH_2OH group involved in the complex with Mo^{VI} was also found enough different for two **A** type isomers (70.1 ppm, $\mathbf{A_1}$ isomer and 72.9 ppm, $\mathbf{A_2}$ isomer, respectively) and thus can be used for determination of the complex type (Table 1).

In the ^1H NMR spectrum of a freshly prepared solution of D-*erythro*-L-*manno*-octitol (not shown), a high concentration of Mo^{VI} ions resulted in a relatively large half width of the signals and thus a low resolution in the spectra. Nevertheless, the proton signals due to the CH_2OH group at δ 4.37 and 4.08, suggesting the presence of the $\mathbf{A_1}$ isomer, were clearly dominant. However, in the COSYDQF spectrum the number of the cross peaks was doubled for each of the abovementioned signals. Consequently, two sets of data were obtained: one ascribable to the C-1–C-8 spin system of the whole molecule and the other one in which the C-5–C-8 part showed identical chemical shifts as C-1–C-4. The latter one suggested the presence of a highly symmetric $\mathbf{A_1}$–$\mathbf{A_1}$ bis-dinuclear molybdate complex, which rather surprisingly precipitated quickly from the solution and these changes could be observed in the ^1H

Table 1
^{1}H and ^{13}C NMR data of D-*erythro*-L-*manno*-octitol and D-*erythro*-L-*gluco*-octitol in bis-dinuclear tetradentate molybdate complexes [a]

Saccharide	C-1–C-4 region complex type and isomer	Chemical shifts δ (ppm) or coupling constants J (Hz)												C-5–C-8 region complex type and isomer
δ H		1	1′	2	3	4	5	6	7	8	8′			
manno-Octitol	A_2	**4.58–4.42**		**≈4.88**	**4.81**	**4.53**	**4.67**	**4.92**	**4.77**	**4.37**	**4.08**			A_1
	A_1	**4.08**	**4.36**	**4.82**	**5.18**	**4.66**	**4.66**	**5.18**	**4.82**	**4.36**	**4.08**			A_1
gluco-Octitol	Q	**4.27**	**4.11**	**4.38**	**4.67**	**4.40**	**4.64**	**4.78**	**4.96**	**4.38**	**4.08**			A_1
		4.27	**4.11**	**4.38**	**4.67**	**4.40**	[c]	[c]	[c]	**4.50**	**4.50**			A_2
		1	1′				2	3	4	5	5′			
Arabinitol		3.90	3.76				**4.54**	**4.65**	**4.75**	**4.35**	**4.07**			A_1
		3.72	3.72				**4.31**	**4.73**	**4.85**	**4.50**	**4.50**			A_2
$^{3}J_{H,H}$]		1,2	1′,2	1,1	2,3	3,4	4,5	5,6	6,7	7,8	7,8′	8,8′	6,8′	
manno-Octitol	A_2	[c]	[c]	[c]	[c]	[c]	<1	0.6	4.4	<1	2.6	10.1	2.0	A_1
	A_1	<1	2.6	10.1	4.4	<1	<1	<1	4.4	<1	2.6	10.1	2.0	A_1
gluco-Octitol	Q	c	2.3	9.3	<1	<1	9.3	<1	4.4	<1	2.4	11.6	1.9	A_1
Arabinitol			1′,2	1,1			1,2	2,3	3,4	4,5	4,5′	5,5′	3,5′	
			5.3	11.2			8.2	0.8	4.4	0.2	2.6	10.3	2.0	A_1
			[c]	[c]			[c]	0.2	4.2	1.3	4.4	[c]		A_2
δ C		1		2	3	4	5	6	7	8				
manno-Octitol	A_2	**72.8**		**82.4**	**91.4**	**77.2**	**82.4**	**83.5**	**91.5**	**69.9**				A_1
	A_1	**70.1**		**91.7**	**83.3**	**80.1**	**80.1**	**83.3**	**91.7**	**70.1**				A_1
gluco-Octitol	Q	**76.8**		**84.1**	**82.6**	**84.0**	**81.1**	**92.0**	**83.6**	**70.2**				A_1
		1					2	3	4	5				
Arabinitol [b]		63.8					**82.8**	**82.9**	**91.5**	**70.1**				A_1
		64.6					**78.6**	**91.0**	**82.5**	**72.9**				A_2

[a] Chemical shifts of CH protons and carbon atoms involved in the complex are in bold.
[b] Data taken from Ref. 9.
[c] Signal not resolved.

NMR spectra (Fig. 1). During the precipitation, the concentration of Mo^{VI} ions decreased and the resolution of the spectra improved. Thus, the presence of the second type of bis-dinuclear molybdate complexes became more evident. On the basis of its characteristic chemical shifts and coupling constants (Table 1), it was found that the carbon chain adopted the sickle–sickle arrangements also in this case, however, with the $\mathbf{A_1}$ isomer in one part and the $\mathbf{A_2}$ isomer in the other part of the molecule. In this $\mathbf{A_1}$–$\mathbf{A_2}$ bis-dinuclear molybdate complex, the signals due to H-4 and H-5 (δ 4.53 and 4.67, Table 1) were singlets ($^3J_{4,5} < 1$ Hz) and no NOE effect was detected between them. Such negligibly small coupling constants correspond to the stereochemical arrangement where the dihedral angle between H-4 and H-5 is around 90° or 270° (Scheme 1). This fact suggests that two dinuclear molybdate cores participate in the chelation with **3** to form the $\mathbf{A_1}$–$\mathbf{A_2}$ bis-dinuclear complex, however, they are separated from each other. Furthermore, NMR data show that two separated dinuclear molybdate cores in $\mathbf{A_1}$–$\mathbf{A_2}$ complex undergo the rearrangement creating a new aggregation of octahedra. The latter leads to the formation of the symmetric $\mathbf{A_1}$–$\mathbf{A_1}$ complex that precipitates from the solution. An NMR spectrum collected before the end of the precipitation process is seen in Fig. 1(C). Only a very small amount of the $\mathbf{A_1}$–$\mathbf{A_2}$ complex could be detected and signals due to the $\mathbf{A_1}$–$\mathbf{A_1}$ complex are missing in the spectrum. Therefore, only signals characteristic of the dinuclear tetradentate complex of the *galacto* arrangement (sickle) remained in the spectrum (Table 1).

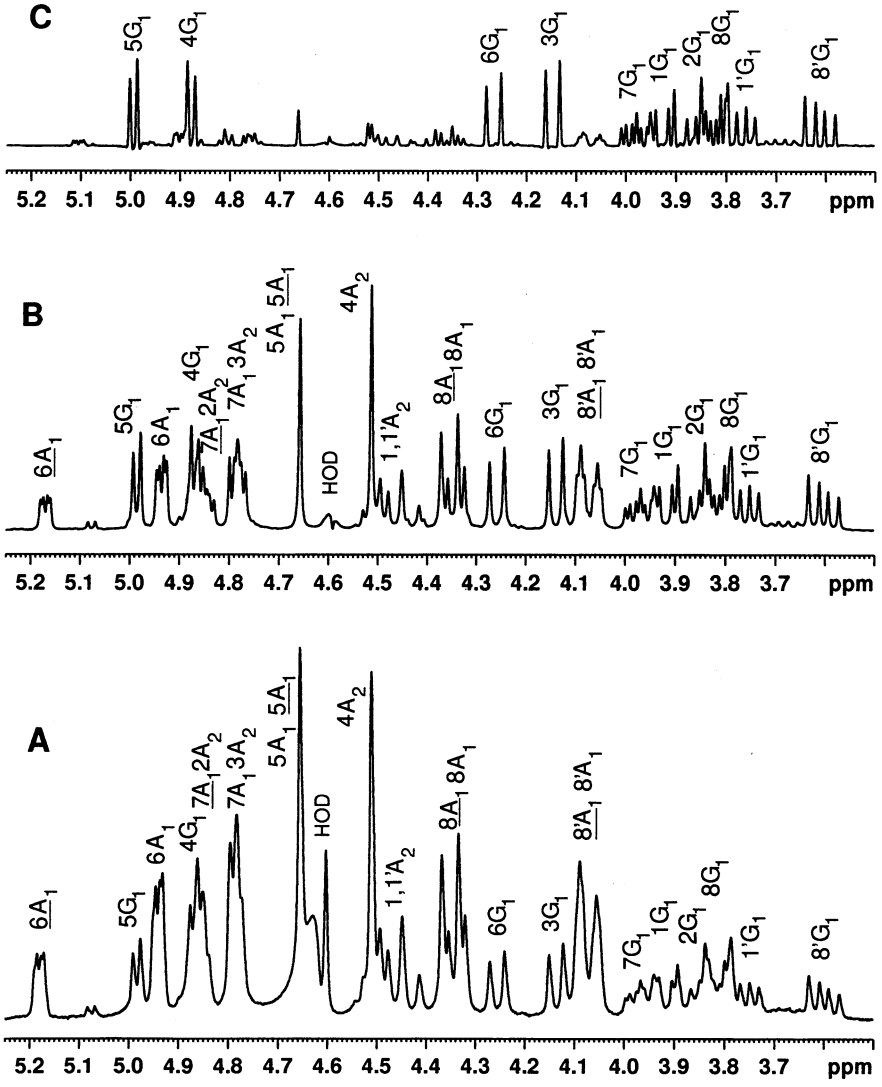

Fig. 1. 300 MHz ^{1}H NMR spectra of D-*erythro*-L-*manno*-octitol in aqueous solution of ammonium molybdate (1:4) at 310 K. (A) Spectrum measured immediately after preparation of the complex solution; (B) after 1 h; (C) after 4 h. Signals due to the complex with the *galacto* arrangement became dominant after the precipitation of the $\mathbf{A_1}$–$\mathbf{A_1}$ complex. Signals due to the precipitated A_1–A_1 complex are underlined.

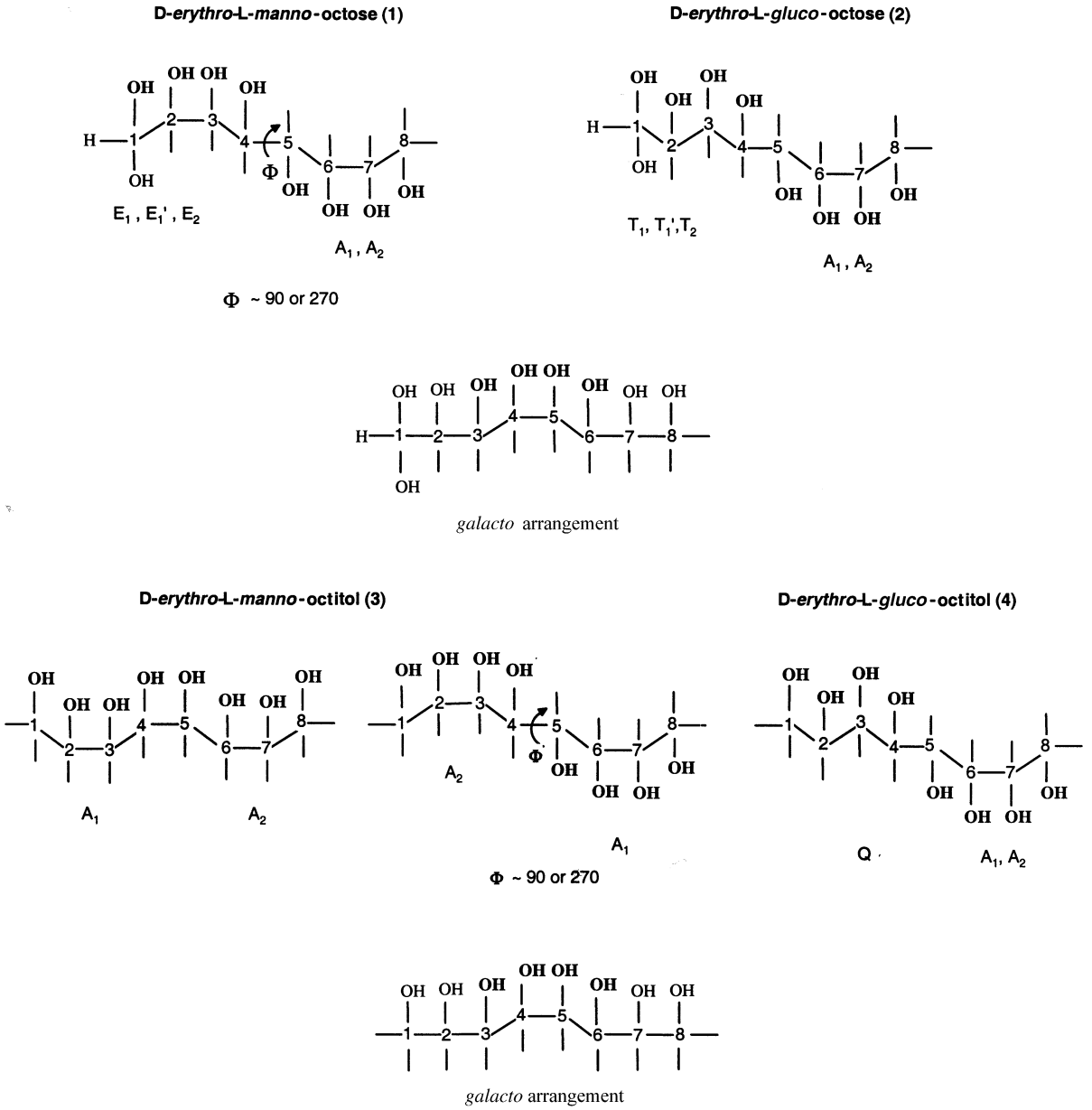

Scheme 1. Arrangements of the carbon chain of D-*erythro*-L-*manno*-octose (**1**), D-*erythro*-L-*gluco*-octose (**2**), D-*erythro*-L-*manno*-octitol (**3**) and D-*erythro*-L-*gluco*-octitol (**4**) in the identified bis-dinuclear tetradentate molybdate complexes.

The precipitated $\mathbf{A_1}$–$\mathbf{A_1}$ complex was further characterized by solid state NMR spectroscopy and its ^{13}C CP MAS NMR spectrum with a tentative assignment is shown in Fig. 2(A). The spectrum corresponds to the highly symmetric structure of this bis-dinuclear complex of **3** as only four broad signals, corresponding to two parts of the molecule (C-1–C-4 and C-5–C-8), are seen in the spectrum. However, only an X-ray analysis could give more details about the structure of the bis-dinuclear molybdate core formed in this complex. A ^{13}C CP MAS NMR spectrum of the dinuclear tetradentate complex of mannitol[21] (Fig. 2(B)) is shown for comparison as well. Signals were assigned on the basis of the NMR data of this complex in aqueous solution.

Recently, it was found that the spatial arrangement of alditol complex with the *xylo* site as the donor (**Q** type complex) was zig-zag and large signal half widths were characteristic for it in both ^1H NMR and ^{13}C NMR spectra.[5] Consequently, any coupling constants could be extracted and the assignment of signals was only tentative.[5] D-*erythro*-L-*gluco*-Octitol (**4**) presents *xylo* and *arabino* sites suitable for the chelation at C-1–C-4 and C-5–C-8 parts of the molecule, respectively. According to previous observations, the C-1–C-4 part of D-*erythro*-L-*gluco*-octitol molecule was found to be involved in the **Q** type complex with the zig-zag spatial arrangement of the carbon chain and no isomer was detected for this complex (Table 1). Contrary to **Q**

type complexes of lower alditols, the signals originating from the C-1–C-4 part were much narrower and thus several coupling constants could be extracted from the ^{1}H NMR spectra (Table 1). In the C-5–C-8 part of the molecule with the *arabino* site, two isomers $\mathbf{A_1}$ and $\mathbf{A_2}$ were identified as expected (Table 1). Signals H-4 and H-5 (δ 4.40 and 4.64) were found as doublets ($^3J_{4,5}$ 9.3 Hz) indicating either syn- or antiperiplanar dispositions between both tetradentate binuclear complexes. However, the antiperiplanar disposition between **Q** and **A** parts of the molecule was inferred from the fact that no NOE effect was detected between H-4 and H-5 in 1D and 2D NOESY spectra.

In spite of ideal *erythro–erythro* and *threo–erythro* arrangements of **3** and **4**, a small amount of the dinuclear tetradentate complex, including OH groups at C-3, C-4, C-5 and C-6 of the *galacto* site, was formed (Table 2, Fig. 1). The complexes with the *galacto* arrangement of OH groups were already shown to be the most stable.[5,10] In the case of perseitol, this type of complex was found in two isomeric forms $\mathbf{G_1}$ and $\mathbf{G_2}$, both showing characteristic NMR shifts. The values of chemical shifts and coupling constants of the latter

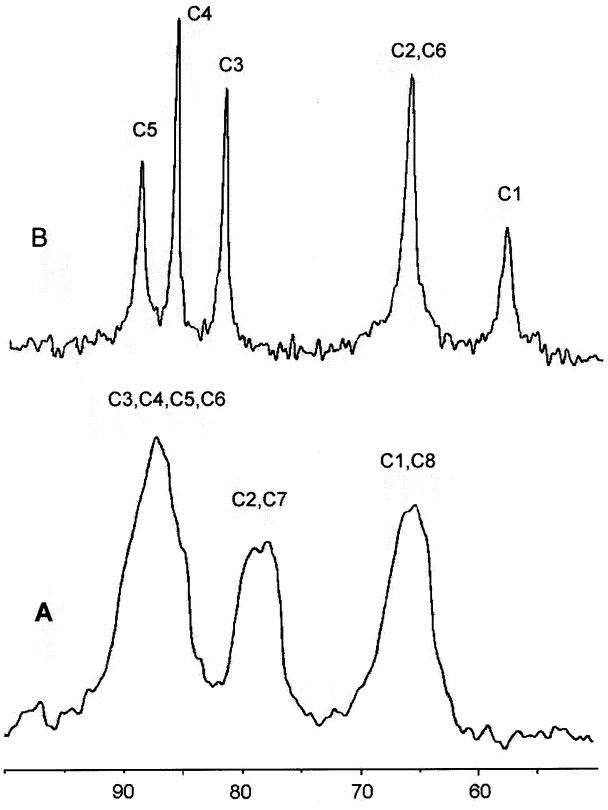

Fig. 2. Solid state ^{13}C CP MAS NMR spectra of the precipitated bis-dinuclear tetradentate $\mathbf{A_1}$–$\mathbf{A_1}$ complex of D-*erythro*-L-*manno*-octitol (A) and the dinuclear tetradentate complex of mannitol (B).[21] The signals assignments are only tentative based on the HSQC spectrum of mannitol complex[21] in aqueous solution.

isomeric forms are given (Table 2) for a comparison with the data of **3** and **4**.

In general, both pyranoid and furanoid forms of aldoses prevail in aqueous solution, with traces of acyclic hydrated and aldehyde forms. Formation of different amounts of various dinuclear Mo^{VI} complexes of acyclic hydrated forms of aldoses were found in previous studies.[4,6] The complex, in which the hydrated aldehyde group and its three vicinal OH groups are involved, is supposed to be very close to the active one which is responsible for epimerization. This type of complex, in the form of two isomers, was found to be formed with aldotetroses and 5-deoxy-aldopentoses, which are present in the aqueous solution in the furanose form.[7] $\mathbf{E_1}$ and $\mathbf{E_2}$ isomers with the sickle arrangement were detected for erythrose and 5-deoxy-ribose. On the other hand, $\mathbf{T_1}$ and $\mathbf{T_2}$ isomers with the zig-zag arrangement of the carbon chain were found for threose and 5-deoxy-arabinose. Each isomer showed characteristic chemical shifts ^{1}H and ^{13}C NMR spectra (Tables 3 and 4). In the ^{1}H NMR spectra also the values of coupling constants $^3J_{1,2}$ and $^3J_{2,3}$ were indicative for each type of complex e.g., $\mathbf{E_1}$ $\delta \approx 5.43$, $^3J_{1,2}$ 0.6–0.9, $^3J_{2,3}$ 4.4; $\mathbf{E_2}$ $\delta \approx 5.77$, $^3J_{1,2} \approx 0.2$; $\mathbf{T_1}$ $\delta \approx 5.48$, $^3J_{1,2} < 1$; $\mathbf{T_2}$ $\delta \approx 5.59$, $^3J_{1,2}$ 2.2, $^3J_{2,3}$ 0.2.

Contrary to erythrose, lyxose and mannose displayed preferably the molybdate complex **F** in the furanose form (donor OH groups at C-1, C-2, C-3 and C-5) showing characteristic H-1 and C-1 chemical shifts at δ 6.21 and 112.7, respectively.[11] For both, less than 5% of the $\mathbf{E_1}$ isomer was detected.[4] However, in the case of D-*glycero*-L-*manno*-heptose the amount of the **F** complex decreased to about 20% and complexes of the acyclic structure prevails with 15% of the $\mathbf{E_1}$, $\mathbf{E_2}$ and 15% of the $\mathbf{G_1}$, $\mathbf{G_2}$ isomers. Less than 5% of the **F** complex was found in the solution of D-*erythro*-L-*manno*-octose **1**, while complexes of the acyclic hydrated form were found dominant.

NMR spectra of octoses showed resonances corresponding not only to the chelated compound but to the free pyranose and furanose forms as well. The hydrated acyclic form of D-*erythro*-L-*manno*-octose **1** and D-*erythro*-L-*gluco*-octose **2** showed similar structural features as **3** and **4**, respectively. Consequently, formation of the $\mathbf{A_1}$ and $\mathbf{A_2}$ isomers of binuclear tetradentate complex at the *arabino* site (with the sickle arrangement of the carbon chain) was found in the C-5–C-8 part of the molecule of both **1** and **2**. NMR data of $\mathbf{A_1}$ and $\mathbf{A_2}$ isomers formed in C-5–C-8 part of the molecule of both **1** and **2** are in a good agreement with the data of arabinitol (Tables 3 and 4). In the anomeric region of the NMR spectra, the H-1/C-1 chemical shifts at δ 5.40/95.3 and δ 5.79/98.9 (Tables 3 and 4) suggested the formation of $\mathbf{E_1}$ and $\mathbf{E_2}$ isomers (sickle arrangement), respectively, in the C-1–C-4 part of **1** in accord with the *lyxo* homomorphous series configuration. In the case of **2**, the configuration of the *xylo* homomorphous

Table 2
^{1}H and ^{13}C NMR data of D-*erythro*-L-*manno*-octitol, D-*erythro*-L-*gluco*-octitol and perseitol in the *galacto* type dinuclear tetradentate molybdate complex [a]

Saccharide		Complex type	Chemical shifts δ (ppm) or coupling constants J (Hz)										
	δ H		1	1′	2	3	4	5	6	7	7′ or 8	8′	
Perseitol [b]		G_1	3.70	3.70	**4.32**	**4.75**	**4.98**	**4.27**	3.98	3.83	3.60		
		G_2	[c]	[c]	**4.52**	**4.70**	**4.89**	**4.19**	3.80	[c]	[c]		
manno-Octitol		G_1	3.93	3.78	**3.86**	**4.16**	**4.89**	**5.00**	4.27	3.99	3.83	3.62	
gluco-Octitol		G_1	3.90	3.67	**3.90**	**4.24**	**4.77**	**4.96**	4.27	3.98	3.83	3.60	
	$^{3}J_{H,H}$		1,2	1′,2	1,1	2,3	3,4	4,5	5,6	6,7	7,8	7,8′	8,8′
Perseitol [b]		G_1	[c]	[c]	[c]	**<1**	**4.5**	<1	**9.2**	2.9	6.7	11.2	
		G_2	[c]	[c]	[c]	**<1**	**4.5**	<1	**8.5**	[c]	[c]	[c]	
manno-Octitol		G_1	3.8	5.5	11.1	8.5	<1	**4.3**	<1	**8.9**	3.7	6.5	11.0
gluco-Octitol		G_1	3.2	6.0	12.0	7.3	<1	**4.4**	<1	**9.2**	2.8	6.6	12.0
	δ C		1	2	3	4	5	6	7	8			
Perseitol [b]		G_1	64.7	**78.7**	**91.1**	**82.8**	**81.8**	71.8	64.4				
		G_2	63.8	**82.6**	**83.0**	**91.1**	**79.2**	72.8	64.7				
manno-Octitol		G_1	64.9	73.1	**79.5**	**91.3**	**83.0**	**81.9**	71.9	64.5			
gluco-Octitol		G_1	64.5	73.0	**79.6**	**91.3**	**82.8**	**81.9**	71.8	63.6			

[a] Chemical shifts of CH protons and carbon atoms involved in the complex are in bold.
[b] Data taken from Ref. [5].
[c] Signal not resolved.

Table 3
^{1}H NMR chemical shifts of acyclic hydrated forms of aldoses in dinuclear (tetroses–heptoses) and bis-dinuclear (octoses) tetradentate molybdate complexes [a]

Saccharide	C-1–C-4 region complex type [c]	Chemical shifts δ (ppm)									C-5–C-8 region complex type [c]
		1	2	3	4	4′ or 5	5′ or 6	6′ or 7	7′ or 8	8′	
D-Erythrose [b]	E_1	**5.40**	**4.65**	**4.83**	**4.49**	**4.45**					
	E_2	**5.79**	**4.74** [d]	**4.85** [d]	[e]	[e]					
D-Mannose	E_1	**5.45**	**4.71**	**5.01**	**4.33**	**3.98**	3.90	3.73			
	E_2	**5.81**	[e]	[e]	[e]	[e]	[e]				
D-*glycero*-L-*manno*-Heptose	E_1	**5.43**	**4.65**	**4.95**	**4.34**	**3.86**	3.73	3.66			
	E_2	**5.77**	[e]	[e]	[e]	[e]	[e]	[e]			
D-*erythro*-L-*manno*-Octose [c]	E_1	**5.47**	**4.69**	**4.92**	**4.64**	**4.63**	**4.89**	**4.78**	**4.36**	**4.08**	A_1
	E_1'	**5.46**	**4.73**	**5.12**	**4.49**	**4.49**	**4.78**	**4.85**	**4.49**	**4.49**	A_2
	E_2	**5.72**	[e]	[e]	[e]	[e]	[e]	[e]	[e]	[e]	
D-Threose [b]	T_1	**5.46**	**4.24**	**4.24**	[e]	[e]					
	T_2	**5.58**	**4.12**	**4.08**	**4.25**	**4.10**					
D-Glucose	T_1	**5.48**	**4.12** [d]	**4.40** [d]	**4.25** [d]	[e]					
	T_2	**5.60**	[e]	[e]	[e]	[e]					
D-*glycero*-L-*gluco*-Heptose	T_1	**5.48**	**4.14** [d]	**4.38** [d]	**4.27** [d]	[e]	[e]	[e]			
	T_2	**5.59**	[e]	[e]	[e]	[e]	[e]	[e]			
D-*erythro*-L-*gluco*-Octose	T_1	**5.51**	**4.29**	**4.42**	**4.33**	**4.63**	**4.85**	**4.76**	**4.37**	**4.08**	A_1
	T_1'	**5.53**	**4.29**	**4.48**	**4.34**	**4.40**	**4.76**	**4.85**	**4.40**	**4.40**	A_2
	T_2	**5.58**	**4.17**	[e]	[e]	[e]	[e]	[e]	[e]	[e]	

[a] Chemical shifts of CH protons and carbon atoms in the complex are in bold.
[b] Data taken from Ref. 7.
[c] Region defines carbon atoms OH groups of which are involved in the tetradentate complex.
[d] Assignment of signals within a data set of a given aldose may be interchanged.
[e] Not assigned or not resolved signals.

Table 4
^{13}C NMR chemical shifts of acyclic hydrated forms of aldoses in dinuclear (tetroses–heptoses) and bis-dinuclear (octoses) molybdate complexes [a]

Saccharide	C-1–C-4 region complex type and isomer [b]	Chemical shifts δ (ppm)								C-5–C-8 region complex type and isomer [b]
		1	**2**	**3**	**4**	**5**	**6**	**7**	**8**	
D-Erythrose	E_1	**95.3**	**94.1**	**81.6**	**72.5**					
	E_2	**98.9**	**90.0** [c]	**88.0** [c]	**69.9**					
D-Mannose	E_1	**95.4**	**94.0**	**81.9**	**81.2**	71.8	64.4			
	E_2	[d]	[d]	[d]	[d]	[d]	[d]			
D-*glycero*-L-*manno*-Heptose	E_1	**95.3**	**94.0**	**81.9**	**80.4**	69.8[c]	71.6[c]	64.4		
	E_2	**98.8**	[e]	[e]	[e]	[e]	[e]	[e]		
D-*erythro*-L-*manno*-Octose	E_1	**95.5**	**94.2**	**82.1**	**79.4**	**80.3**	**82.9**	**91.7**	**70.2**	A_1
	E'_1	**95.6**	**94.3**	**82.0**	**81.9**	**77.3**	**91.5**	**82.5**	**72.9**	A_2
	E_2	**98.7**	**90.1**	**87.8**	[d]	[d]	[d]	[d]	[d]	
D-Threose	T_1	**99.7**	**86.0**	**81.1**	**76.2**					
	T_2	**98.2**	**83.4**	**76.8**	**76.2**					
D-Glucose	T_1	**99.7**	**86.8**	**80.8**	**85.1**	71.2	64.4			
	T_2	**98.3**	[e]	[e]	[e]	[e]	[e]			
D-*glycero*-L-*gluco*-Heptose	T_1	**99.7**	**86.8**	**80.9**	**84.0**	71.6	67.8	64.5		
	T_2	**98.2**	**83.4**	[e]	[e]	[e]	[e]	[e]		
D-*erythro*-L-*gluco*-Octose	T_1	**99.7**	**86.8**	**83.1**	**81.1**	**80.4**	**82.9**	**91.8**	**70.4**	A_1
	T'_1	**99.9**	**85.5**	**82.9**	[e]	**77.0**	**91.6**	**82.7**	**73.1**	A_2
	T_2	**98.4**	**84.2**	[e]	[e]	[e]	[e]	[e]	[e]	

[a] Chemical shifts of carbons OH group of which is involved in the complex are in bold.
[b] Region defines carbon atoms OH groups of which are involved in the tetradentate complex.
[c] Assignment of signals within a data set of a given aldose may be interchanged.
[d] Not detected signals due to a very low concentration.
[e] Not assigned.

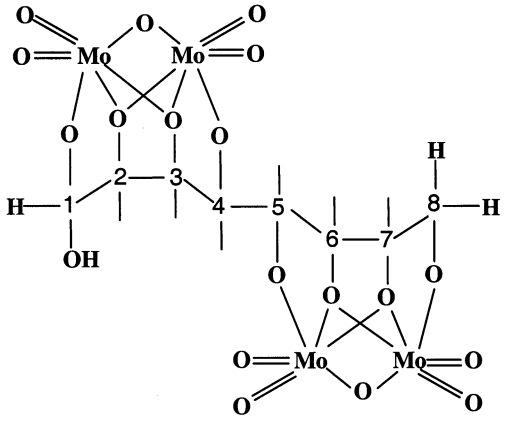

Scheme 2. Representation of the chelation of the D-*erythro*-L-*manno*-octose (**1**) by vicinal hydroxyls of aldose, in bis-dimolybdate complex.

series at C-1–C-4 was reflected in the formation of $\mathbf{T_1}$ and $\mathbf{T_2}$ isomers with the zig-zag arrangement: H-1/C-1 δ 5.51/99.7 and δ 5.58/98.4, respectively. However, due to the formation of $\mathbf{A_1}$, $\mathbf{A_2}$ isomers in the C-5–C-8 part, two sets of chemical shifts for $\mathbf{E_1}$ and $\mathbf{T_1}$ (denoted $\mathbf{E_1}$, $\mathbf{E'_1}$ and $\mathbf{T_1}$, $\mathbf{T'_1}$) were identified. The H-1/C-1 chemical shifts of $\mathbf{E'_1}$ and $\mathbf{T'_1}$ δ 5.46/95.6 and 5.53/99.9, respectively, are very close to those of $\mathbf{E_1}$ and $\mathbf{T_1}$. Thus, at the ratio of $\mathbf{A_1}$:$\mathbf{A_2}$ = 2:1, the following ratios of $\mathbf{E_1}$:$\mathbf{E'_1}$:$\mathbf{E_2}$ = 6:3:1 and $\mathbf{T_1}$:$\mathbf{T'_1}$:$\mathbf{T_2}$ = 6:3:1 were found. The presence of $\mathbf{E'_2}$ and $\mathbf{T'_2}$ isomers could not be confirmed owing to low intensities of the $\mathbf{E_2}$ and $\mathbf{T_2}$ isomers. NMR data for bis-dinuclear Mo^{VI} complexes formed by **1** and **2** are listed in Tables 3 and 4.

The value of vicinal coupling constant between H-4 and H-5 ($^3J_{4,5} < 1$ Hz) indicated that the dihedral angle between both dinuclear tetradentate complexes is close to 90° or 270° in D-*erythro*-L-*manno*-octose. The value of $^3J_{4,5}$ was found comparable with that in D-*erythro*-L-*manno*-octitol ($^3J_{4,5} < 1$ Hz) and suggests that both **1** and **3** have similar stereochemical arrangements in the complex with molybdate ions.

It was recently found that one-bond proton–carbon coupling constants ($^1J_{CH}$) were larger for atoms that are directly bound with their corresponding counterparts in the complex with respect to data for the uncomplexed compound.[9] Magnitudes for $^1J_{CH}$ (Table 5) found for **2** were consistent with these findings, although small differences exist among the $^1J_{CH}$ values. Slightly larger differences were observed for C-3–H-3 and C-7–H-7 couplings and variations among other couplings in complexed and uncomplexed compounds were smaller. In any case, larger $^1J_{CH}$ magnitudes in the complexed compounds **2** indicate that $^1J_{CH}$ magnitudes might be used as parameters to determine the complexation sites in molybdate complexes.

In all cases, remarkable changes in the chemical shifts values of particular protons and carbons could be observed for individual pairs of isomers (Tables 3 and 4). This fact, together with the observed deshielding pattern, lead to the conclusion about the reverse way of binding of binuclear molybdate core.[7,8,12] Its asymmetry, well documented in the X-ray analysis of erythritol dinuclear molybdate complex,[22] supported this hypothesis.

A steric hindrance of the lateral substituents R^1 and R^2 linked to carbons of the central complexed core of the ligand (R^1 represented by H and R^2 by lateral carbon chain) was suggested as an explanation of the formation of two alditol isomers involving the central *erythro* diol groups.[9,12] Isomers having R^1 and R^2 substituents oriented away from the chelation site were indicated to be more stable as compared with complexes involving steric hindrance. Nevertheless, in aldooctitols **3** and **4** no different lateral substituent was present and formation of isomers was detected. Moreover, the precipitation of the $\mathbf{A_1}$–$\mathbf{A_1}$ bis-dinuclear molybdate complex from solution and the presence of $\mathbf{A_1}$–$\mathbf{A_2}$ as the second most stable complex of **3** were observed. In the case of D-*erythro*-L-*manno*-octose bis-dinuclear complex, according to this hypothesis, the formation of $\mathbf{E_1}$ and $\mathbf{E_2}$ isomers (C-1–C-4 part) could be eventually caused by steric hindrance of the free OH group at C-1 due to hydrated carbonyl group (not involved in the complex) and formation of a second dinuclear Mo^{VI} complex at C-5–C-8 (Scheme 2). This is not very probable. In contrast, results of NOE measurements suggest considerable steric hindrance between the C-1–C-4 and C-5–C-8 parts of the carbon skeleton in both **2** and **4** complexes caused by the size of both dinuclear molybdate cores. Moreover, due to the isomer formations in the C-5–C-8 part of the molecule, $\mathbf{E_1}$–$\mathbf{A_1}$ and $\mathbf{E_1}$–$\mathbf{A_2}$ bis-dinuclear Mo^{VI} complexes (Tables 3 and 4) were identified. All these facts suggest that the origin of the isomer formations should be mainly in the reverse way of binding of asymmetric binuclear molybdate core.

The present data extend our knowledge on the formation of complexes between aldooctoses and molybdate ions. It appears that the stereochemistry of carbohydrate Mo^{VI} complexes depends both upon the appropriate number and configuration of hydroxyl groups available for the complex formation. High-resolution NMR data of these complexes further show that each form, i.e., cyclic and acyclic, of carbohydrate molecule can originate in different types of molybdate complexes.

Acknowledgements

This research was supported in part by VEGA grant No. 2/2002/22 awarded by the Slovak Academy of Sciences.

Table 5
Comparative $^{1}J_{C,H}$ coupling constants in acyclic hydrated forms of aldoses involved in bis-dinuclear tetradentate molybdate complexes and in pure D-*erythro*-L-*gluco*-octose in aqueous solution

	C-1–C-4 region complex type [a]	Coupling constants $^{1}J_{C,H}$ (Hz)							C-5–C-8 region complex type[a]
		C-1,H-1	C-2,H-2	C-3,H-3	C-4,H-4	C-5,H-5	C-6,H-5	C-7,H-7	
Mo^{VI} complexes of									
D-*erythro*-L-*manno*-Octose	E_1	165.1	151.2	150.6	147.2	147.9	150.7	149.5	A_1
	E_1'	166.2	151.8	150.2	147.1	147.3	149.7	149.6	A_2
	E_2								
D-*erythro*-L-gluco-Octose	T_1	169.1	150.3	147.2	149.0	146.1	150.0	145.4	A_1
	T_1'	171.1	148.4	[c]	[c]	143.3	150.6	147.4	A_2
	T_2	168.5	148.8	[c]	[c]	[c]	[c]	[c]	
Pure aldose [b]									
D-*erythro*-L-gluco-Octose	β	170.2	142.0	137.5	145.6	142.5	[c]	141.2	
	α	161.5	148.2	141.5	[c]	145.6	[c]	142.1	

[a] Region defines carbon atoms OH groups of which are involved in the tetradentate complex.
[b] $^{1}J_{CH}$ of D-*erythro*-L-*manno*-octose were not obtained due to the highly overlapped signals.
[c] Not resolved signals.

References

1. Bílik, V. *Chem. Zvesti* **1972**, *26*, 183–186, 187–189, 372–375.
2. Hayes, M. L.; Pennings, N. J.; Serianni, A. S.; Barker, R. *J. Am. Chem. Soc.* **1982**, *104*, 6764–6769.
3. Clark, E. L., Jr.; Hayes, M. L.; Barker, R. *Carbohydr. Res.* **1986**, *153*, 263–270.
4. Bílik, V.; Matulová, M. *Chem. Papers* **1990**, *44*, 257–265.
5. Matulová, M.; Bílik, V.; Alföldi, J. *Chem. Papers* **1989**, *43*, 403–414.
6. Matulová, M.; Bílik, V. *Chem. Papers* **1990**, *44*, 77–87.
7. Matulová, M.; Bílik, V. *Chem. Papers* **1992**, *46*, 253–256.
8. Matulová, M.; Bílik, V. *Carbohydr. Res.* **1993**, *250*, 203–209.
9. Chapelle, S.; Verchère, J. F.; Sauvage, J. P. *Polyhedron* **1990**, *9*, 1225–1234.
10. Chapelle, S.; Verchère, J. F. *Carbohydr. Res.* **1991**, *211*, 279–286.
11. Sauvage, J. P.; Chapelle, S.; Verchère, J. F. *Carbohydr. Res.* **1992**, *237*, 23–32.
12. Verchère, J. F.; Chapelle, S.; Xin, F.; Crans, D. C. *Prog. Inorg. Chem.* **1998**, *47*, 837–945.
13. Bílik, V.; Alföldi, J.; Matulová, M. *Chem. Papers* **1986**, *40*, 763–771.
14. Davies, L. A.; Laue, E. A.; Keeler, J.; Moskau, D.; Lohman, J. *J. Magn. Reson.* **1991**, *94*, 637–644.
15. Stott, K.; Keeler, J.; Van, Q. N.; Shaka, J. *J. Magn. Reson.* **1997**, *125*, 302–324.
16. Schleucher, J.; Schwendinger, M.; Sattler, M.; Schedletzky, O.; Glaser, S. J.; Sörensen, O. W.; Griesinger, C. *J. Biomol. NMR* **1994**, *4*, 301–306.
17. Zhu, G.; Renwick, A.; Bax, A. *J. Magn. Reson. Series A* **1994**, *110*, 257–261.
18. Uhrínová, S.; Uhrín, D.; Liptaj, T.; Bella, J.; Hirsch, J. *Magn. Reson. Chem.* **1991**, *29*, 912–922.
19. Mehring, M. *High-Resolution NMR Spectroscopy in Solids*; Springer: New York, 1976.
20. Sauvage, J. P.; Chapelle, S.; Donna, A. M.; Verchère, J. F. *Carbohydr. Res.* **1993**, *243*, 293–305.
21. Hedman, B. *Acta Crystallogr., Sect. B* **1977**, *33*, 3077–3083.
22. Ma, L.; Liu, S.; Zubieta, J. *Polyhedron* **1989**, *8*, 1571–1573.